Langmuir–Blodgett Films Composed of Cationic Amphiphile Complexed with Triblock Polyanion with a Biomembrane-Mimicking, Channellike Pathway for Transporting Ions

Masazo Niwa,* Akihiro Mukai, and Nobuyuki Higashi

Department of Applied Chemistry, Faculty of Engineering, Doshisha University, Kamikyo-ku, Kyoto 602, Japan

Received October 2, 1990; Revised Manuscript Received January 2, 1991

ABSTRACT: Novel polyion-complexed Langmuir–Blodgett (LB) films having a channellike pathway for transporting ions were prepared from the polyion-complexed monolayers composed of newly synthesized triblock polyanions (poly(styrene-*p*-sulfonate)-*block*-poly(methacrylic acid)-*block*-poly(styrene-*p*-sulfonate) ($S_nM_mS_n$)) and a double-chain, cationic amphiphile. The cationic amphiphile was found to complex preferentially with poly(styrene-*p*-sulfonate) segments and not with poly(methacrylic acid) segments at low pH. The polyion complexes formed stable surface monolayers, which were affected by pH in the subphase. The permeability of the hydrophilic permeants (KCl and tetramethylammonium bromide) across the LB films of those monolayers (10 layers) was reversibly switched on and off by pH change as a result of the conformational change of the poly(methacrylic acid) segments, while the permeability of the hydrophobic permeant (hexyltrimethylammonium bromide) with long alkyl chain was controlled by the phase transition of the component monolayers rather than by pH change.

Introduction

Biological membranes consist of the lipid bilayer and protein molecules capable of transporting specific substrates across the membranes. The protein molecules may undergo reversible conformational changes to make a channel in the membrane for the specific substrate transported. If one could develop an artificial membrane that would possess such a channel function in biomembranes, it would be useful not only for biomimetic model systems of ion transport but also for practical applications in sensors and separations. Recently, a biomembrane model from a synthetic macromolecule, which has the polypeptide microdomain as a membrane protein model, has been prepared and has worked as a permeability-controllable membrane by the conformational change of polypeptide segment.[1]

Langmuir–Blodgett (LB) films would be good candidates for a biomembrane model due to their resemblance in structural and physicochemical properties to the lipid bilayer membrane. In fact, the substrate permeability across LB films has been successfully controlled by the phase transition between crystal and liquid crystal of the component monolayer similar to the lipid bilayer function.[2] An attempt to improve the long-term thermal and mechanical stability of LB films is, however, required for most practical applications. Research efforts on LB films consisting of polymeric monolayers are rapidly expanding.[3,4] Polyion complexation of ionic amphiphiles and oppositely charged polyions at the air–water interface is one of the most fascinating techniques for stabilization and facilitated deposition of monolayers.[5,6] Such polyion-complexed LB films have been found to be stable enough in water as a permeation barrier.[7,8] Cast films of the polyion complexes, which have fundamentally a similar layer structure to the LB films, have been reported to control the substrate permeability through them by the phase transition of membrane components.[9] We have focused on the incorporation of a conformation-changeable polymer segment as a channel model of biomembranes into the polyions and on the control of substrate permeability in the polyion-complexed LB films. In a previous report,[10] we showed the preliminary result of KCl transport across the LB films (10 monolayers) composed of poly(styrene-*p*-sulfonate)-*block*-poly(methacrylic acid)-*block*-poly(styrene-*p*-sulfonate) ($S_nM_mS_n$)/1 polyion complexed monolayer whose structural formula is shown in Figure 1. $S_nM_mS_n$/1 complexes formed well-behaved surface monolayers that were affected by pH change in the subphase due to the conformational transition of poly(methacrylic acid) (PMMA) segments in $S_nM_mS_n$ triblock polyions. These PMAA segments in LB films were suggested to function as a permeating pathway for KCl. The present paper will describe the results of our more intensive study on the pH-induced permeation control of a series of $S_nM_mS_n$/1 polyion-complexed LB films. We employed tetramethylammonium bromide (C_1N^+) and hexyltrimethylammonium bromide (C_6N^+) with different molecular size and hydrophobicity from KCl as permeants in order to elucidate which portion of the LB films they mainly pass through.

Experimental Section

Materials. Double-chain ammonium salt 1 was prepared as follows according to the literature.[11] The condensation of L-glutamic acid with myristyl alcohol was carried out and the diester thus obtained was reacted with ω-bromoundecanoyl chloride and then treated with trimethylamine. The structure and purity of the final product were confirmed by ^{1}H NMR (JEOL, JNM-GX400 FTNMR spectrometer) spectrum, TLC with flame ionization detection (Yatron Laboratories, Tokyo), and elemental analysis (C, H, and N). Methacrylic acid, ethanol, methanol, and benzene were purified by the usual methods. Other chemicals used were of analytical grade.

Preparation of Triblock Polyions ($S_nM_mS_n$). Triblock polyions ($S_nM_mS_n$) were prepared according to the manner reported previously.[12] The radical polymerization of methacrylic acid was carried out upon UV irradiation (low-pressure Hg lamp) in a sealed glass ampule at 30 °C with bis(isopropylxanthogen) disulfide (BX) as initiator–transfer agent–terminator[12] and ethanol as solvent. After a definite period of time, the ampule was opened, and the content was poured into a large excess of benzene. The precipitate was purified by reprecipitation from ethanol (solvent) and benzene (nonsolvent) and freeze-dried. The number-average degree of polymerization (m) of the polymers was determined by VPO (Knauer vapor-pressure osmometer) in ethanol. The contents of xanthate groups incorporated into the polymer were determined from UV spectra (Shimadzu UV-2100 spectrophotometer, Kyoto; λ_{max} = 284 nm: $\pi \rightarrow \pi^*$ transition of

0024-9297/91/2224-3314$02.50/0

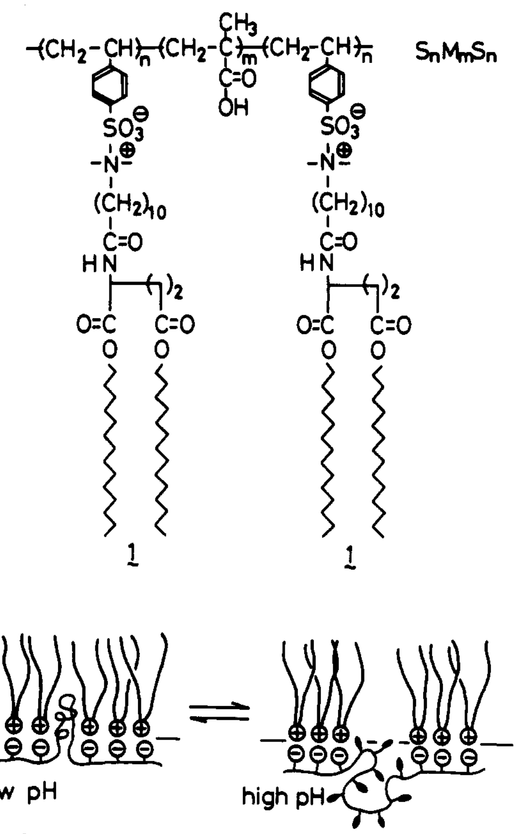

Figure 1. Structure of polyion complex composed of polyanion ($S_nM_mS_n$) and cationic amphiphile (1) and a model for the conformational change in the form of surface monolayers.

SC(=S)O, ϵ_{max} = 1.13 × 10^4 L mol^{-1} cm^{-1}). Subsequently, the block polymerization of sodium styrene-*p*-sulfonate was carried out upon UV irradiation in the same way with PMAA containing xanthate groups at each end of polymer chain as macrophotoinitiator obtained above and water as solvent. After polymerization, the content of the ampule was poured into a large excess of methanol, and then the precipitate was purified by reprecipitation from water (solvent) and methanol (nonsolvent) and freeze-dried. The average degree of polymerization (*n*) of blocking sodium styrene-*p*-sulfonate was determined by estimating the contents of methacrylic acid units in polymer by a conductometric titration with aqueous NaOH. The polymerization conditions and characterization of polymers thus obtained were summarized in Table I.

Preparation of Polyion Complexes ($S_nM_mS_n/1$). An aqueous solution of 1 (15 mM) was obtained by sonication for a few minutes with a Branson Sonifier II 250. Equivalent amounts of an aqueous dispersion of 1 (15 mM) and an aqueous solution of $S_nM_mS_n$ (15 unit mM) were mixed at an appropriate pH. The precipitates were washed with water and acetone several times and then dried in vacuo to give a white powder. The stoichiometric composition of these polyion complexes was determined by ^1H NMR and elemental analysis. Anal. Calcd for $S_{10}M_{13}S_{10}/1$: C, 68.81; H, 10.42; N, 2.79. Found: C, 68.59; H, 10.74; N, 2.66. Calcd for $S_{10}M_{34}S_{10}/1$: C, 67.74; H, 10.14; N, 2.56. Found: C, 67.39; H, 10.54; N, 2.40.

Spreading Experiments. The monolayers were obtained by spreading of benzene–methanol (8/2 in volume) solutions of $S_nM_mS_n/1$ complexes on purified water ("Milli Q" system, Millipore Ltd.). The concentration of the spreading solution was 1.0 mg mL^{-1}. Ten minutes after spreading, the gaseous monolayer was compressed continuously. The compressional velocity was 1.20 cm^2 s^{-1}. Below this value, the effect of compression rate on the monolayer area was within experimental error. Wilhelmy's plate (filter paper plate) method and a Teflon-coated trough with a microprocessor-controlled film balance (San-Esu Keisoku Ltd., Fukuoka) with a precision of 0.01 mN m^{-1} were used for surface pressure measurements. The measurements of surface pressure (π)–area (*A*) curves for all samples were repeated several times to check their reproducibility. The pH in the subphase was adjusted with either NaOH or HCl as required. Langmuir–Blodgett multilayers were prepared by means of a microprocessor-controlled film balance, FSD-21 (San-Esu Keisoku Ltd., Fukuoka). The dipping speed of a substrate was kept constant at 15 mm min^{-1} for both downward and upward strokes. Multilayers could be deposited on various materials, such as quartz plate and a porous polycarbonate film (Nuclepore, pore size 0.2 μm, Nomura Micro Science Co., Ltd.).

Table I
Polymerization and Characterization of Triblock Polyions ($S_nM_mS_n$)

	telechelic PMAA[a]			$S_nM_mS_n$[e]		
run	feed comp,[b] $[MAA]_0/[BX]_0$	N_x[c]	*m*[d]	feed comp,[f] $[xanthate]_0/[SS]_0$	yield, %	*n*[g]
1	3.0	2.1	13	0.050	45	10
2	5.0	2.0	34	0.025	25	10

[a] Photopolymerizations were carried out in ethanol at 30 °C.
[b] $[BX]_0$: concentration of bis(isopropylxanthogen) disulfide; $[MAA]_0$ = 3.0 mol L^{-1}.
[c] Number of isopropyl xanthate groups per polymer molecule calculated by the following equation: $N_x = M_n(\mathrm{Abs}/\epsilon C)$; ϵ = 1.13 × 10^4 L mol^{-1} cm^{-1} λ_{max} = 284 nm); *C*, concentration of polymer (g L^{-1}); Abs, absorbance at 284 nm; M_n, number-average molecular weight of polymer determined by VPO in ethanol.
[d] Number-average degree of polymerization (*m*) calculated by the following equation: $m = (M_n/M_{MAA})(1 - [M_x(\mathrm{Abs}/\epsilon C)]$; M_x, molecular weight of isopropyl xanthate group[b], M_{MAA}, molecular weight of MAA.
[e] Photopolymerizations were carried out in water at 30 °C.
[f] $[xanthate]_0$, concentration of xanthate groups at both ends of PMAA chain; $[SS]_0$ = 1.00 mol L^{-1}.
[g] Number-average degree of polymerization (*n*) calculated by the following equation: $n = [(10^3/\theta - M_{MAA})m - M_xN_x]/2M_{SS}$; θ, the content of MAA unit in triblock polymer (mmol g^{-1}); M_{SS}, molecular weight of SS.

Permeation. Permeation experiments were performed between pure water (14 cm^3) and aqueous KCl, C_1N^+, or C_6N^+ (50 mM, 57 cm^3) with a conventional, thermostated, H-shaped cell. The film area was 0.79 cm^2, and both sides of the cell were stirred at a constant speed. Permeation of salts (KCl, C_1N^+, and C_6N^+) was followed by detecting increases in the electrical conductance in the water side, since good linear correlations between the conductance and the concentration of salts were obtained in the range 0.1–50 mM. The calibration equations between conductance and concentration of salts were as follows: concentration of KCl (M) = 6.25 × conductance (S) and concentration of ammonium salt (C_1N^+ or C_6N^+) (M) = 8.0 × conductance (S). Apparent permeation rates, *P* (cm s^{-1}), were calculated from eq 1 where *k*, *v*, *a*, and C_0 are the initial slope of the salt concentration

$$P = kv/aC_0 \qquad (1)$$

in the water side versus time curve (mol cm^{-3} s^{-1}), the volume of the water side of the cell (14 cm^3), the film area (0.79 cm^2), and the concentration of permeants in the salt solution side (50 mM), respectively. LB films were treated for 20 min with an acidic (HCl) or alkaline (NaOH) solution with a prescribed pH at room temperature and then were set in the permeation cell. The salt permeability across the LB films was measured in pure water (pH 6.8). The permeation experiment for the bare Nuclepore was also performed at pH 6.8 in the same way.

Results and Discussion

Preparation and Composition of the Polyion Complexes ($S_nM_mS_n/1$). We have shown in previous papers[12] that BX behaves as an effective photoinitiator–transfer agent–terminator for the polymerization of vinyl monomers upon UV irradiation and that telechelic polymers containing an isopropyl xanthate group as a photosensitive moiety at each end of the polymer chain can be readily prepared. When a second vinyl monomer was polymerized in the presence of those macrophotoinitiators upon UV irradiation, BAB-type triblock polymers were formed. In the polymerization system, each segment length (*m*, *n*) of

Table II
Chemical Composition of Polyion Complexes Prepared at Different pHs

polyion	pH	comp of polyion complex,[a] [1]/[SS]
$S_{10}M_{13}S_{10}$	3.9	0.97/1
	8.7	1.32/1
PSS	6.5	0.96/1

[a] Composition of polyion complexes were estimated by ^1H NMR as follows. The ratio ([1]/[SS]) of 1 to SS group in triblock polyanion was calculated by using the area ratio of the signal of ω-CH_3 in 1 to that of C_6H_4 (phenyl) in the polyion.

the blockpolymers was sufficiently controllable by the concentration of initiators and the conversion of monomers. In the same manner, triblock polyions, $S_nM_mS_n$, consisting of a PMAA segment and poly(styrene-*p*-sulfonate) (PSS) segments were newly prepared (Table I). At first, telechelic PMAAs with different chain length (m = 13, 34) containing a photosensitive isopropyl xanthate group at each end of the polymer chain were prepared by photopolymerization of MAA in the presence of BX. Sodium styrene-*p*-sulfonate was then polymerized by those photosensitive PMAAs as a macrophotoinitiator upon UV irradiation. As a result, two types of triblock polyions ($S_{10}M_{13}S_{10}$ and $S_{10}M_{34}S_{10}$) were obtained as shown in Table I. Polyion complexes ($S_nM_mS_n$/1) were prepared by mixing equivalent amounts of an aqueous dispersion of 1 (15 mM) and an aqueous solution of $S_nM_mS_n$ (15 mM total units) at pHs 3.9 and 8.9. The chemical composition of the $S_{10}M_{13}S_{10}$/1 complex, a typical sample, thus obtained was estimated by ^1H NMR and summarized in Table II, in which the data for PSS/1 complex was included for comparison. The ratio of the content of 1 to that of styrene-*p*-sulfonate (SS) groups in the triblock polyanion ([1]/[SS]) was calculated by using the area ratio of the signal of ω-CH_3 in 1 to that of C_6H_4 (phenyl) in the polyanion. When the complex was prepared at pH 8.7, at which carboxyl groups of PMAA segment in $S_{10}M_{13}S_{10}$ might be ionized since the apparent dissociation constant (pK_a) of PMAA was reported to be pK_a 7.3,[13] the ratio of [1] to [SS] was [1]/[SS] = 1.32/1; i.e., the cationic amphiphile 1 is suggested to complex not only with PSS segments but also with PMAA segment in $S_{10}M_{13}S_{10}$. On the other hand, the complex obtained at pH 3.9 has a composition of [1]/[SS] = 0.97/1, implying that the cationic amphiphile 1 complexed preferentially with PSS segments of $S_{10}M_{13}S_{10}$ triblock polymer and not with PMAA segment. Similar results were obtained for the complexation of 1 with $S_{10}M_{34}S_{10}$ triblock polymer. It has been reported that the proton resonance of NCH_3 in the NMR spectrum of the PSS/dodecyltrimethylammonium bromide polyion complex exhibits an upfield shift compared with that in solution containing dodecyltrimethylammonium bromide only due to the ring-current effect of the aromatic groups.[12] In the case of our polyion complexes prepared at pH 3.9, such ring-current shifts were also observed. The proton resonance of NCH_3 (3.4 ppm) in a $CDCl_3$ solution of 1 shifted upfield to 3.0 ppm upon complexation with $S_nM_mS_n$. This result suggests both the complete removal of unreacted, free 1 and the preferential complexation of 1 with PSS segments and not with PMAA segment. From these NMR data and the results of the elemental analysis (see Experimental Section), the structure of polyion complexes ($S_nM_mS_n$/1) prepared at pH 3.9 was confirmed to be that as shown in Figure 1. Thus, the polyion complexes prepared at pH 3.9 were used in the following experiments.

Surface Monolayers. Figure 2 shows the π–A isotherms of a 1:1 $S_{10}M_{34}S_{10}$/1 complex prepared at pH 3.9, on water ([NaCl] = 0.1 M) at different pH values, 20 °C. At low surface pressure, as expected, molecules lie on the water surface, occupying a large area. With increasing surface pressure, they begin to associate and orient their hydrophobic tails. Following a partially condensed state, there is a transition to a solid state at a transition pressure of ca. 35 mN m^{-1}. At surface pressures below this transition, in particular, π–A curves largely changed depending on the pH of the subphase. Similar situations were observed for the monolayer of $S_{10}M_{13}S_{10}$/1 complex. The pH dependence of the area at a constant pressure of 20 mN m^{-1} (A_{20}) is shown in Figure 3, in which data for the monolayer of PSS/1 complex were included for comparison. In the case of the $S_{10}M_{13}S_{10}$/1 monolayer, the A_{20} value increased discontinuously at around pH 8, which corresponds to the apparent dissociation constant pK_a of PMAA (pK_a 7.3), due to expansion of the monolayer when the pH of the subphase increased. This pH-induced expansion of the monolayer may be ascribed to the dissociation of carboxylic acid groups of the PMAA segment, which should cause a conformational change of the PMAA chain between a globular coil and an expanded conformation as shown schematically in Figure 1. Further drastic increase of the A_{20} value responding to pH was observed in the case of the $S_{10}M_{34}S_{10}$/1 monolayer with a longer PMAA segment. Thus, such a discontinuous expansion of the monolayer by pH change is considered to be related to the PMAA segment length of complexes, similar to the results in the multilayer state as described later. On the other hand, the PSS/1 monolayer was not affected by the pH of the subphase due to the absence of the PMAA segment.

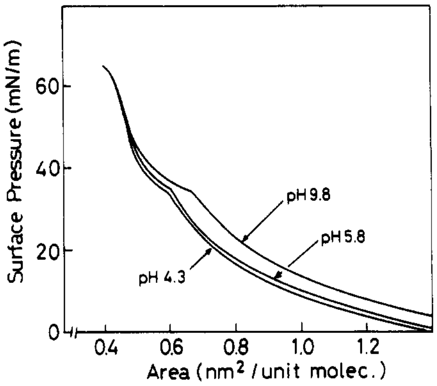

Figure 2. Surface pressure (π)–area (A) isotherms of $S_{10}M_{34}S_{10}$/1 complex on water ([NaCl] = 0.1 M) at different pHs, 20 °C.

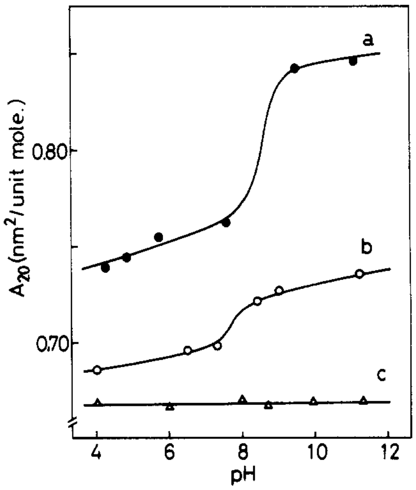

Figure 3. pH dependence of A_{20} value for $S_{10}M_{34}S_{10}$/1 (a), $S_{10}M_{13}S_{10}$/1 (b), and PSS/1 (c) monolayers at 20 °C.

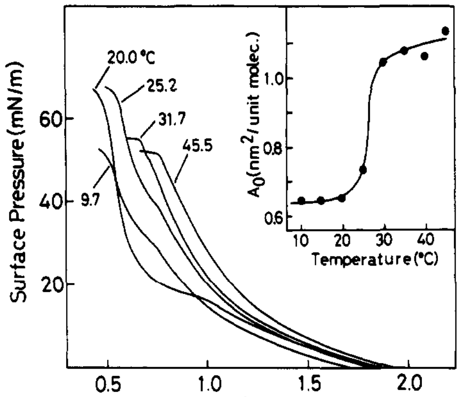

Figure 4. Temperature dependence of π–A curves of $S_{10}M_{13}S_{10}/1$ monolayers. Inset shows the plot of A_0 value against temperature.

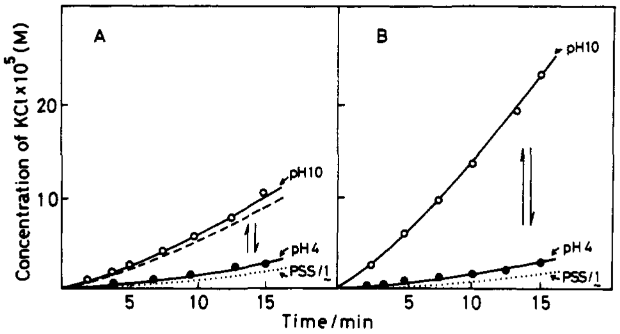

Figure 5. Time–transport curves of KCl across the $S_{10}M_{13}S_{10}/1$ LB film (A) and $S_{10}M_{34}S_{10}/1$ LB film (B) in pure water (pH 6.8) at 20 °C after 20 min of treatment at the prescribed pH. Dashed line and dotted line indicate the data for bare Nucleopore and for the PSS/1 LB film, respectively.

In order to reveal the phase transition properties of monolayers, π–A isotherms of $S_{10}M_{13}S_{10}/1$ were measured at various temperatures (10–50 °C), and the limiting area (A_0), estimated by extrapolating the steepest region to zero pressure, is plotted against temperature in Figure 4. The A_0 value increased drastically near 25 °C, which corresponds to the phase transition temperature of the monolayer from the solid analogue to the liquid analogue.

pH-Dependent Permeability to KCl. Deposition of the monolayers onto one side of a porous polycarbonate film was performed at a surface pressure of 30 mN m^{-1}, 20 °C, on an acidic aqueous solution (pH 4). The substrate was supported by a Teflon plate and thus the transfer ratio could not be determined. The formation of a Y-type multilayer, which means that a monolayer can be deposited onto a substrate during both downward and upward strokes, was evident, however, since the decrease in the surface area was the same during downward and upward strokes for each complexed monolayer. The number of deposited layers was kept constant at 10 layers because it has been found that 10 layers are sufficient to cover all the pores in the substrate film for a similar polymeric LB film.[7,8] Figure 5 displays time–transport curves of KCl across the LB films of $S_{10}M_{13}S_{10}/1$ and $S_{10}M_{34}S_{10}/1$ pretreated at a prescribed pH for 20 min. Figure 5 also includes the permeation data of PSS/1 LB films (10 layers). The PSS/1 LB film did not show a marked difference in KCl permeability between pH 4 and pH 10, as expected, and provided a high barrier capability for KCl permeation. In the case of $S_{10}M_{13}S_{10}/1$ LB film and $S_{10}M_{34}S_{10}/1$ LB film, KCl permeation was considerably suppressed and was close to that for PSS/1 LB film when the LB films were treated at pH 4. In contrast, at pH 10, the KCl permeation was obviously enhanced. In particular, the KCl permeation rate for $S_{10}M_{34}S_{10}/1$ LB film is observed to be ca. 2 times higher than that for the bare substrate. We do not have any conclusive evidence so far to explain this phenomenon, but one interesting possible explanation, which will require further exploration, is that the hydrophilicity of PMAA segments in the LB film increases upon treatment at pH 10. As the result, the dissolution of KCl on the outer film surface and KCl diffusion through the PMAA segment domains formed in the inner film become easier compared with those for the bare, hydrophobic substrate, in spite of the latter's porosity. Anyway, such an enhancement of KCl permeation strongly depends on the PMAA segment length (m): the extent of permeation enhancement for $S_{10}M_{34}S_{10}/1$ LB film upon pH change was larger than that for $S_{10}M_{13}S_{10}/1$ LB film. These results suggest that the pH-dependent permeability change of KCl is due to the conformational change of PMAA segment brought about by the dissociation of carboxyl groups, responding to pH, and that KCl may pass through predominantly the PMAA segment portion in multilayers. When the LB films were again treated at pH 4, the KCl permeation reverted to the original value. Such treatments were repeatable at least four times with good permeation reproducibility.

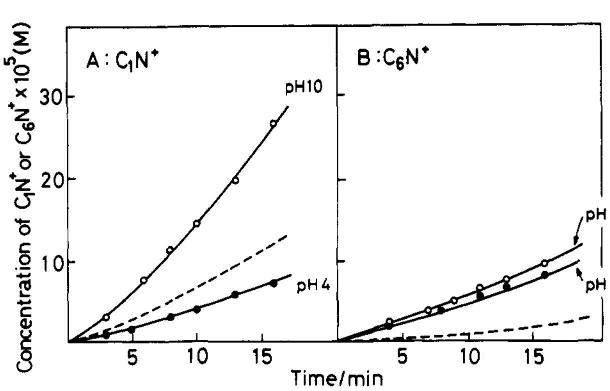

Figure 6. Time–transport curves of C_1N^+ (A) or C_6N^+ (B) across the $S_{10}M_{34}S_{10}/1$ LB film in pure water (pH 6.8) at 20 °C after 20 min of treatment at the prescribed pH. Dashed line shows the data for the bare Nucleopore.

Hydrophobicity of Permeants. In order to elucidate which portion of LB films the permeants mainly pass through, we employed two permeants, C_1N^+ and C_6N^+, which have different hydrophobicities. Figure 6 shows time-transport curves of C_1N^+ and C_6N^+ across the $S_{10}M_{13}S_{10}/1$ LB film at 20 °C after 20-min treatment at a prescribed pH. In the case of C_1N^+, the permeability was markedly varied by pH change, similar to the case of KCl permeation. In contrast, when one used the relatively hydrophobic permeant, C_6N^+, containing long alkyl chain, the permeability was little affected by pH change. Further, the permeability across the LB film was observed to be larger than that across the bare substrate. This phenomenon is also not easily explained, but one plausible explanation is that because of the hydrophobicity of C_6N^+ it penetrates the multilayer and in fact concentrates in the multilayer so that the concentration gradient across the substrate becomes greater than that in the case of the bare substrate itself. From these results, it can be suggested that the permeant C_6N^+ has a different pathway in the LB films from that for C_1N^+ and KCl due to a difference in their hydrophobicity. If C_6N^+ would permeate preferentially a hydrophobic portion of the LB films, the permeability should be affected by a phase transition of the component monolayer (1). In order to test this postulate, the effect of temperature on the permeation

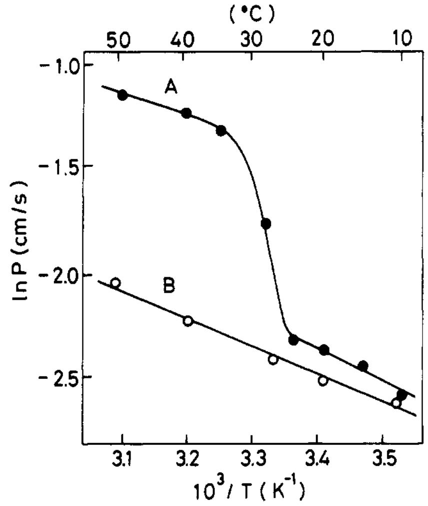

Figure 7. Arrhenius plots of permeation of C_6N^+ probe through (A) $S_{10}M_{13}S_{10}/1$ LB film and (B) bare Nucleopore.

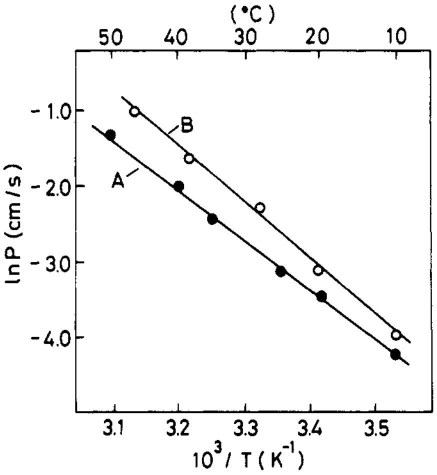

Figure 8. Arrhenius plots of permeation of C_1N^+ probe through (A) $S_{10}M_{13}S_{10}/1$ LB film and (B) bare Nuclepore.

rates was examined. Figures 7 and 8 show Arrhenius plots of the apparent permeation rate, P (cm s^{-1}), of C_6N^+ and C_1N^+ across the $S_{10}M_{13}S_{10}/1$ LB films at pH 6.8. The Arrhenius plots of the bare substrates provided the usual straight lines for both permeants. For the permeation of the hydrophobic C_6N^+ through the LB film, the Arrhenius plot gave a discontinuous jump (five times enhancement) at 25-30 °C, which corresponds to the phase transition temperature (25 °C) obtained from the temperature dependence of π–A curves (Figure 4). Such a permeation rate jump has been observed for the other LB films composed of a bilayer-forming amphiphile.[4] Thus, it is evident that the permeability of C_6N^+ through the LB films was controlled by the phase transition of domains of 1 from solid analogue to liquid analogue. In the case of the C_1N^+ permeation, on the other hand, the Arrhenius plot gave the usual straight line. The PMAA segments in LB films might be partially ionized in this pH region (pH 6.8). This means that the hydrophilic C_1N^+ permeation through the $S_{10}M_{13}S_{10}/1$ LB films is not affected by the phase transition, and C_1N^+ is suggested to permeate predominantly a hydrophilic, partially ionized PMAA segment region of the complexed LB film. From the results obtained above, we can conclude that the permeability of C_6N^+ across the $S_nM_mS_n/1$ LB films is controllable by the phase transition of the membrane component (1) domains and that of hydrophilic permeants (C_1N^+ and KCl) is switched on and off by pH change.

Conclusion

The present study demonstrates that (i) triblock polyion complexes containing a free PMAA segment in the backbone polymer form condensed monolayers that are affected by varying pH in the subphase, (ii) the permeability of the hydrophilic permeants (KCl and C_1N^+) across the LB films of these triblock polyion complexes (10 layers) was reversibly switched on and off by pH change as a result of the conformational change of the PMAA segment, and (iii) the permeability of the hydrophobic C_6N^+ with a long alkyl chain was controlled by the phase transition of the component monolayers. We believe that these findings provide a first example of the preparation of ultrathin, permeability-controllable molecular films that takes advantage of the conformational change of a polyelectrolyte and that such polyion-complexed LB films are of particular significance not only in view of their applicability for sensors and separations but also in view of their resemblance to the channel function in biomembranes.

References and Notes

(1) (a) Maeda, M.; Kimura, M.; Hareyama, Y.; Inoue, S. *J. Am. Chem. Soc.* **1984**, *106*, 250. (b) Higuchi, S.; Mozawa, T.; Maeda, M.; Inoue, S. *Macromolecules* **1986**, *19*, 2263.
(2) Kajiyama, T.; Kumano, A.; Takayanagi, M.; Kunitake, T. *Chem. Lett.* **1984**, 915.
(3) (a) Albrecht, O.; Lashewsky, A.; Ringsdorf, H. *Macromolecules* **1984**, *17*, 937. (b) Lashewsky, A.; Ringsdorf, H.; Schmit, G.; Schneider, J. *J. Am. Chem. Soc.* **1987**, *109*, 788.
(4) Ariga, K.; Okahata, Y. *J. Am. Chem. Soc.* **1989**, *111*, 5618.
(5) Shimomura, M.; Kunitake, T. *Thin Solid Films* **1985**, *132*, 243.
(6) Higashi, N.; Kunitake, T. *Chem. Lett.* **1986**, 105.
(7) Kunitake, T.; Higashi, N.; Kunitake, M.; Fukushige, Y. *Macromolecules* **1989**, *22*, 485.
(8) Niwa, M.; Matsuyoshi, E.; Higashi, N. *Langmuir* **1989**, *5*, 1256.
(9) Okahata, Y.; Taguchi, K.; Seki, T. *J. Chem. Soc., Chem. Commun.* **1985**, 1122.
(10) Niwa, M.; Mukai, A.; Higashi, N. *Langmuir* **1990**, *6*, 1432.
(11) Kunitake, T.; Nakashima, N.; Hayashida, S.; Yonemori, K. *Chem. Lett.* **1979**, 1413.
(12) (a) Niwa, M.; Matsumoto, T.; Izumi, H. *J. Macromol. Sci.-Chem.* **1987**, *A24*, 567. (b) Niwa, M.; Sako, Y.; Shimizu, M. *J. Macromol. Sci.-Chem.* **1987**, *A24*, 1315. (c) Niwa, M.; Higashi, N.; Shimizu, M.; Matsumoto, T. *Makromol. Chem.* **1988**, *189*, 2187.
(13) Ikawa, T.; Abe, K.; Honda, K.; Tsutida, E. *J. Polym. Sci., Polym. Chem. Ed.* **1975**, *13*, 1505.
(14) Gao, Z.; Kwak, Jan, C. T.; Wasylishen, R. E. *J. Colloid Interface Sci.* **1988**, *126*, 371.

Registry No. 1 (copolymer), 133271-17-7; (MMA)(sodium styrene-*p*-sulfonate) (block copolymer), 133271-18-8; KCl, 7447-40-7; CN^+, 64-20-0; C_6N^+, 2650-53-5.